Available online at www.sciencedirect.com
ScienceDirect
Journal of Power Sources 162 (2006) 464–468
JOURNAL OF POWER SOURCES
www.elsevier.com/locate/jpowsour

Short communication

Gel-cast anode substrates for solid oxide fuel cells

Wen Lai Huang *, Qingshan Zhu, Zhaohui Xie

Multi-Phase Reaction Laboratory, Institute of Process Engineering, Chinese Academy of Sciences, 1 Bei'er Tiao, Zhong Guan Cun, Haidian District, P.O. Box 353, Beijing 100080, People's Republic of China

Received 6 April 2006; received in revised form 12 June 2006; accepted 13 June 2006
Available online 26 July 2006

Abstract

By introducing appropriate amounts of monomer and crosslinker (about 10 wt.% of the 8YSZ and NiO powders), high quality porous NiO–8YSZ substrates for planar solid oxide fuel cells (SOFCs) have been fabricated via a gel-casting process. Due to the initiating effect of the NiO in the slurry, no additional initiator was needed to facilitate methacrylamide (MAM) polymerization. Sintering at 1300 °C for 10 h and subsequent reduction at 700 °C for 3 h resulted in Ni–8YSZ anode substrates with the total porosity above 40 vol.%. The measured conductivity was in good agreement with the calculated value, indicating a homogeneous distribution and good connectivity.

Keywords: Gel-casting; Anode; Solid oxide fuel cell

1. Introduction

Gel-casting is a forming technique with many advantages such as low cost, good product homogeneity, high green strength, and so on [1,2], and has been implemented extensively [3–11]. It was employed to fabricate monoliths of either single components such as Al_2O_3 [3], yttria-stabilized zirconia (YSZ) [4], and $Sr(Bi_{1-x}Nd_x)_8Ti_7O_{27}$ [5], or composites such as Al_2O_3–SiC [6] and Al_2O_3–NiO [7]. By combining this technique with the polymer sponge method, Ramay and Zhang [8] produced porous hydroxyapatite scaffolds. Gel-casting has also been utilized to synthesize homogeneous composite powders such as $Zr_{0.84}Y_{0.16}O_{0.92}$, $Ce_{0.8}Gd_{0.2}O_{1.9}$, $Ce_{0.9}Gd_{0.1}O_{1.95}$, $La_{0.9}Sr_{0.1}Ga_{0.8}Mg_{0.2}O_{2.85}$, $La_2Mo_2O_9$, $La_{0.8}Sr_{0.2}CoO_{3-\delta}$, $La_{0.8}Sr_{0.2}FeO_{3-\delta}$, and NiO–$Ce_{0.8}Sm_{0.2}O_{1.9}$ [9–11].

Inspired by the advantages and generic versatility of the gel-casting method, the present work attempts to planar porous substrates of NiO–8YSZ (8 mol.% Y_2O_3 stabilized ZrO_2) which are usually produced via the tape-casting approach [12]. To our knowledge, the gel-casting method has mostly been exploited to produce dense objects, and its suitability for the fabrication of such porous composite is worth investigating.

* Corresponding author. Tel.: +86 10 62558393; fax: +86 10 62536108.
E-mail address: wlhuang@home.ipe.ac.cn (W.L. Huang).

0378-7753/$ – see front matter © 2006 Elsevier B.V. All rights reserved.
doi:10.1016/j.jpowsour.2006.06.026

2. Experimental

2.1. Starting materials

Starting oxides included a commercial NiO powder with an average diameter of around 1.0 μm (A.R., Beijing Shuangyan Chemical Plant, P.R. China) and a 8YSZ powder with an average diameter of 5.1 μm (A.R., GF Zirconium–Titanium Materials Co., Ltd., P.R. China). Methacrylamide (MAM, 98 wt.%, Lancaster, UK) and *N*,*N*′-methylene-bis-acrylamide (MBAM, A.R., Beijing Chemical Reagents Co., P.R. China) were used as the monomer and the crosslinker, respectively. A poly-acrylic ammonia (PAA, pH ≈ 9) solution was prepared by mixing the poly-acrylic acid (Industrial Grade, $M_w \approx 1000$, Beijing Chemical Plant, P.R. China) with dense ammonia (A.R., 25 wt.%, Beijing Chemical Reagents Co.) in the volume ratio of 1:1, utilized as the dispersant, and the solvent adopted was deionized water (Industrial Grade, Institute of Process Engineering, Chinese Academy of Sciences, P.R. China).

2.2. Gel-casting and subsequent treatments

The suspension was prepared via two steps of ball milling. The initial mixture was prepared using the above-mentioned 8YSZ, MAM, MBAM, water, and PAA solution in the weight

ratios of 1.00:0.23:0.01:0.61:0.02. After ball milling for 12 h, the NiO powder and additional PAA solution was added into the system, whose weight ratios to the original 8YSZ were 1.48 and 0.04, respectively, and a second ball milling was conducted for 24 h. The homogeneous slurry was then poured into a mould and sealed. After heating at 70 °C for 3 h, the slurry gelated completely, and the wet gel was then dried under controlled humidity. The resultant dry gel was subsequently calcined at 400 °C for 10 h to remove the organics and sintered at 1120 °C or 1300 °C for 10 h, at the heating rate of 1 °C min^{-1}. The sintered samples were further reduced at 700 °C for 3 h in dry H_2 (≥99.5 wt.%, Beijing Longhui Gases Co., Ltd., P.R. China) at a flow rate of 20 mL min^{-1}.

2.3. Characterization

Thermal gravimetric analysis/differential scanning calorimetry (TGA/DSC) (STA 449C, Netzsch, Germany) was carried out at a heating rate of 5 °C min^{-1} up to 900 °C for the dry gel to determine the weight change and thermal characteristics. Both the sintering characteristics of the dry gel and the thermal expansion of the sintered sample were measured with a dilatometer (L75/1550, Linseis Messgeraete GmbH, Germany). The phases of the samples were analyzed via X-ray diffraction (XRD) (X'Pert Pro, PANalytical, The Netherlands) from 10° to 90° with a scanning speed of 24° min^{-1}. FE-SEM (JSM-6700F, JEOL, Japan) was employed to observe the morphological features of the samples. The total porosity of the sample was evaluated geometrically, i.e., by measuring the apparent volume and the weight of a sample as adopted in Ref. [13]. The electrical resistance of the reduced samples was measured with a RCL meter (PM 6306, Fluke Co., USA).

3. Results and discussion

3.1. Polymerization

The gel-casting procedure in the present work differs in several aspects from the conventional procedure. Firstly and most apparently, no initiator such as $(NH_4)_2S_2O_8$ [1–4,8,10,11] has been introduced into the slurry, but the system gelated successfully. The initiating mechanism might be related to the existence of Ni^{2+} in the system, similar to the reported polymerization behavior initiated by Ni(II)-containing compounds [14]. This self-initiating behavior simplified the casting procedure, avoiding the possible constituent inhomogeneity and air trapping caused by the manual addition of special initiators. Secondly, due to the high quality of the slurry, neither de-aeration [2,4] nor ultrasonication [3] was necessary, and the resultant gels had smooth surfaces. Finally, the ball milling in the present procedure contained two steps, owing to the differences in the isoelectric points [15], densities and particle size of the NiO and 8YSZ powders. The experiments showed that one-step ball milling could not form a satisfactory suspension, while a two-step procedure alleviated the segregations effectively, and yielded a homogenous slurry.

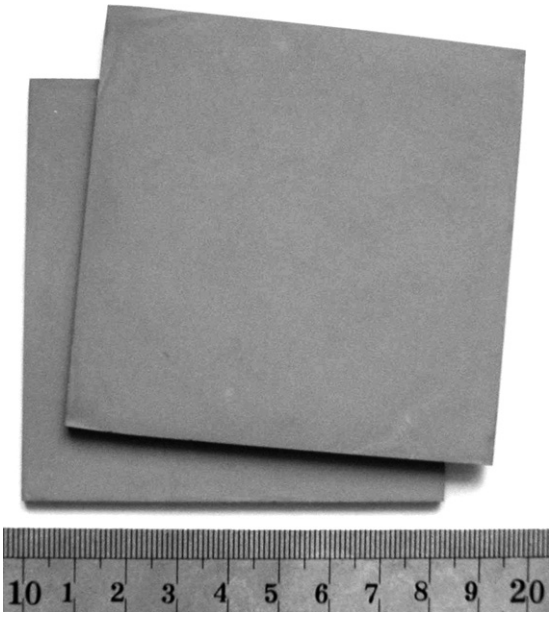

Fig. 1. The appearance of the dry gels.

3.2. Characteristics of the dry gels

The dry gels retained the surface smoothness of the wet gels and the strength was high enough for machining, such as grinding. Fig. 1 illustrates the appearance of some typical dry gels with edges ground manually using SiC sand papers.

FE-SEM images of the dry gels are given in Fig. 2. It is observed that the gel surface (Fig. 2(a)) is microscopically uniform without defects such as pinholes or flaws. It is also found that the dry gel is porous in nature, and this can be better observed on the fractured surface (Fig. 2(b)). A large amount of polymer (which might be poly-methacrylamide, PMAM) can also be observed with a higher resolution (Fig. 2(c)).

The XRD pattern of the dry gel is presented in Fig. 3(bottom). The detected phases are only 8YSZ and NiO, with the grain size of about 30 and 100 nm, respectively, according to the Scherrer calculations.

TGA/DSC results (not shown) indicate that the removal of organics peaks at about 376 °C, and remains until about 470 °C. Sintering curve (not shown) of the dry gel exhibits an expansion around 316 °C corresponding to the organics elimination, and the rapid shrinkage above 915 °C.

3.3. Characteristics of the sintered samples

The XRD pattern of the sample after sintering at 1300 °C for 10 h is illustrated in Fig. 3(top). In comparison with the dry gel, the 8YSZ and NiO grains have grown to about 300 and 380 nm, respectively, due to the sintering process.

The cycling thermal expansion feature of the 1300 °C-sintered sample has been measured up to 1000 °C at a heating/cooling rate of 3 °C min^{-1}, and the obtained coefficient of thermal expansion (CTE) is approximately 12.5×10^{-6} K^{-1} in the temperature range of 600–800 °C, and consistent with the results in Ref. [13]. The thermal expansion was almost reversible

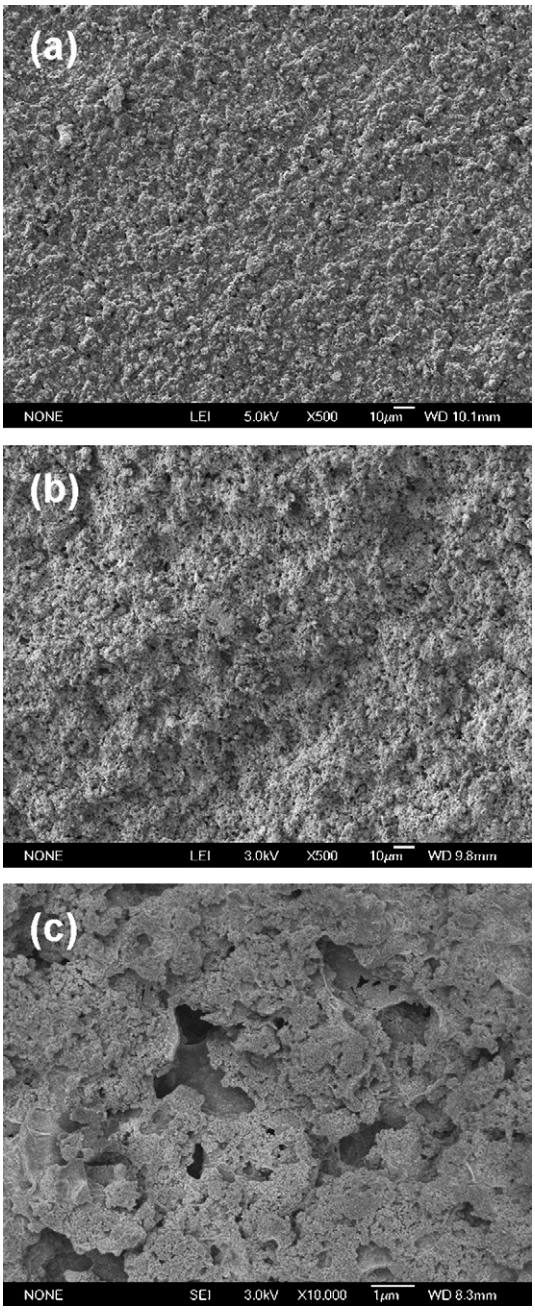

Fig. 2. FE-SEM images of the dry gel on the natural (a) and fractured surfaces (b and c).

in the heating/cooling cycle, suggesting the absence of microscopic cracks.

FE-SEM images of the 1300 °C-sintered sample are given in Fig. 4(a and b). After the organic removal and a sintering shrinkage of over 10%, pores were still obvious, and geometric measurements gave a porosity value of around 27 vol.%. Good adhesion among the particles can be observed, along with apparent growth of grains.

In order to depict the pore evolution during sintering, samples sintered at an intermediate temperature (1120 °C) for 10 h were also investigated. FE-SEM images (not shown) showed that the polymers had been removed, but sintering had not proceeded,

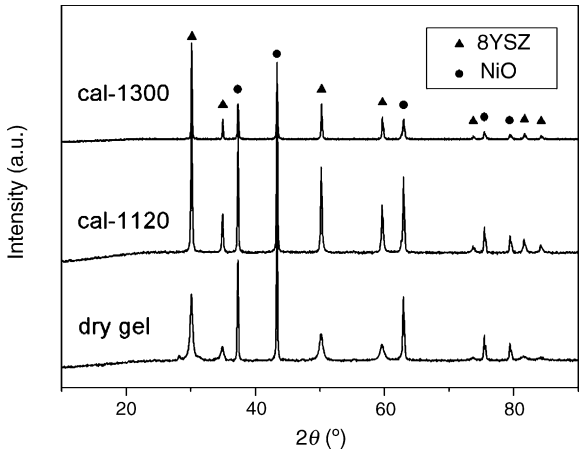

Fig. 3. XRD patterns of the dry gel (bottom) and the samples sintered at 1120 °C (middle) and 1300 °C (top), respectively.

and volumes of pores existed among the particles. The sintering led to about a 1% linear shrinkage from the sintering curve and geometric measurements, and the resultant sample exhibited enough strength for grinding and electrolyte coating (via screen printing or dip coating) with the porosity of around 50 vol.%. Its XRD pattern is shown in Fig. 3(middle), and the Scherrer calculation suggested that the 8YSZ grains had reached about 70 nm while the NiO grains almost retained the original size (around 100 nm).

3.4. Characteristics of the reduced samples

The XRD pattern of the sample sintered at 1300 °C and subsequently reduced at 700 °C is shown in Fig. 5(top). It is found that the NiO has been reduced to Ni completely, and the Ni grains are around 100 nm according to the Scherrer calculator.

FE-SEM images of the reduced sample are shown in Fig. 4(c and d). The comparison with Fig. 4(a and b) makes it clear that the reduction treatment has generated pores in the particle boundaries, and the geometric measurement shows that the total porosity has reached about 45 vol.%. The Ni phase was thus calculated to occupy about 43 vol.% of the solid (excluding the pores) and 24 vol.% of the total sample (including the pores), according to the original ratios in the starting mixtures and confirmed by the weight loss during reduction.

The electrical conductivity of the reduced sample was also measured at room temperature to determine the distributional homogeneity and connectivity of the Ni particles, and the result was in good agreement with the calculated value according to the conductivity of pure Ni and the sample porosity. At room temperature, pure Ni exhibits the resistivity of $7 \times 10^{-8}\ \Omega\,m$ [16] and thus a conductivity of about $1.4 \times 10^{5}\ S\,cm^{-1}$. Considering that the Ni phase is about 24 vol.% of the porous sample, the conductivity of the sample will be derived to be about $3.4 \times 10^{4}\ S\,cm^{-1}$ if the tortuosity factor is neglected (i.e., assigned to be 1). The measured conductivity is about $1.5 \times 10^{4}\ S\,cm^{-1}$, indicating a reasonable tortuosity factor of around 2, and good connectivity of the Ni phase in the composite. For comparison, the sample sintered at 1120 °C for 10 h was also reduced under the

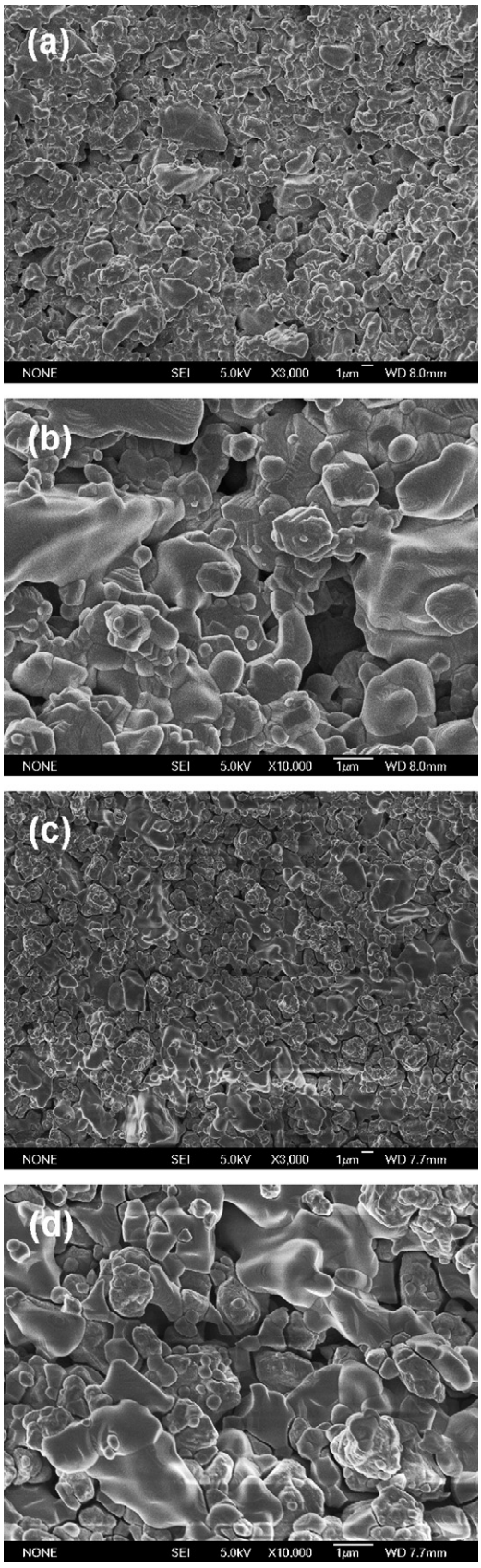

Fig. 4. FE-SEM images of the 1300 °C-sintered (a and b) and subsequently 700 °C-reduced (c and d) samples.

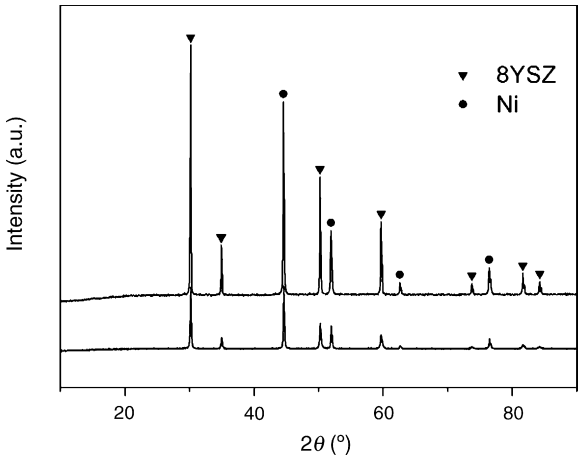

Fig. 5. XRD patterns of the 700 °C-reduced samples after sintering at 1300 °C (top) and 1120 °C (bottom), respectively.

same conditions as the 1300 °C-sintered one. Its XRD pattern (Fig. 5(bottom)) suggests complete reduction of NiO as well. Geometric measurements revealed that its porosity was about 64 vol.%, and the Ni phase was about 14 vol.% of the total sample (including the pores). Hence, the calculated conductivity of this sample is about 2.0×10^4 S cm^{-1} without taking into account the tortuosity factor. However, the measured conductivity is around 7.0 S cm^{-1}, indicating very poor connectivity of the Ni phase.

4. Conclusion

Porous NiO/8YSZ substrates have been fabricated successfully via a gel-casting process. Due to the initiating effect of NiO, no special initiators were introduced into the system. The total porosity of the samples after sintering at 1300 °C for 10 h was around 27 vol.%, and the reduction treatment generated anode substrates with a total porosity of around 45 vol.%. The Ni particles exhibit a homogeneous distribution and good connectivity according to the electrical resistivity measurements of the porous samples. These characteristics show that the as-synthesized samples are suitable for solid oxide fuel cell (SOFC) anode substrates.

Acknowledgement

This work has been financially supported by the National Natural Science Foundation of China (Grant No. 20406023).

References

[1] M.A. Janney, O.O. Omatete, US Patent No. 5,028,362 (1991).
[2] R. Gilissen, J.P. Erauw, A. Smolders, E. Vanswijgenhoven, J. Luyten, Mater. Des. 21 (2000) 251–257.
[3] A.A. Balaluo, M. Kokabi, M. Manteghian, R. Sarraf-Mamoory, J. Eur. Ceram. Soc. 24 (2004) 3779–3787.
[4] X. Liu, G. Li, J. Tong, D. Chen, Ceram. Int. 30 (2004) 2057–2059.
[5] Z.X. Xiong, C. Fang, J.R. Huang, H. Qiu, M. Lin, Mater. Sci. Eng. B99 (2003) 138–142.
[6] S. Ananthakumar, K. Prabhakaran, U.S. Hareesh, P. Manohar, K.G.K. Warrier, Mater. Chem. Phys. 85 (2004) 151–157.

[7] K. Niihara, B.-S. Kim, T. Nakayama, T. Kusunose, T. Nomoto, A. Hikasa, T. Sekino, J. Eur. Ceram. Soc. 24 (2004) 3419–3425.
[8] H.R. Ramay, M. Zhang, Biomaterials 24 (2003) 3293–3302.
[9] A. Tarancón, G. Dezanneau, J. Arbiol, F. Peiró, J.R. Morante, J. Power Sources 118 (2003) 256–264.
[10] J.-G. Cheng, S.-W. Zha, J. Huang, X.-Q. Liu, G.-Y. Meng, Mater. Chem. Phys. 78 (2003) 791–795.
[11] Y. Yin, W. Zhu, C. Xia, G. Meng, J. Power Sources 132 (2004) 36–41.
[12] F. Tietz, H.-P. Buchkremer, D. Stöver, Solid State Ionics 152–153 (2002) 373–381.
[13] A.C. Müller, D. Herbstritt, E. Ivers-Tiffée, Solid State Ionics 152–153 (2002) 537–542.
[14] R. Miyakoshi, A. Yokoyama, T. Yokozawa, J. Am. Chem. Soc. 127 (2005) 17542–17547.
[15] G.A. Parks, Chem. Rev. 65 (1965) 177–198.
[16] http://www.webelements.com.